J Appl Electrochem (2012) 42:737–743
DOI 10.1007/s10800-012-0408-2

ORIGINAL PAPER

Photocatalysis and photoelectrocatalysis using nanocrystalline titania alone or combined with Pt, RuO_2 or NiO co-catalysts

Maria Antoniadou · Paraskevi Panagiotopoulou · Dimitris I. Kondarides · Panagiotis Lianos

Received: 19 January 2012 / Accepted: 31 March 2012 / Published online: 13 April 2012

Abstract Photocatalytic mineralization of ethanol in the presence of oxygen has been studied in aqueous photocatalyst suspensions by employing either pure nanocrystalline titania or TiO_2 combined with Pt, RuO_2 or NiO co-catalysts. Combined photocatalysts demonstrated a diverse behavior. Highest mineralization rates were obtained with Pt/TiO_2 and lowest with RuO_2/TiO_2 and NiO/TiO_2. These results were related with the photocatalysts' behavior when used as photoanodes for the production of electricity in a photoactivated fuel cell running with ethanol as fuel. The highest current was obtained with pure titania. The current dropped in the case of Pt/TiO_2 and became much lower in the case of RuO_2/TiO_2 and NiO/TiO_2 photoanodes. Both current and voltage were lower in the presence of oxygen than in its absence. It is concluded that the presence of electron scavengers, like O_2, and/or the use of efficient photocatalysts, like titania-supported Pt, yield less electric power but assist ethanol mineralization process.

Keywords Photocatalysis · Photoelectrocatalysis · Photofuel cell · Combined photocatalysts · TiO_2 · Pt/TiO_2 · RuO_2/TiO_2 · NiO/TiO_2

M. Antoniadou · P. Lianos
Engineering Science Department, University of Patras, 26500 Patras, Greece

P. Panagiotopoulou · D. I. Kondarides (✉)
Department of Chemical Engineering, University of Patras, 26500 Patras, Greece
e-mail: dimi@chemeng.upatras.gr

P. Lianos (✉)
FORTH/ICE-HT, P.O. Box 1414, 26504 Patras, Greece
e-mail: lianos@upatras.gr

1 Introduction

Photoactivated fuel cells (Photo-Fuel-Cell, PFC) [1] provide an interesting alternative to conventional liquid-fuel cells running on methanol or ethanol, because they possess certain advantages with respect to the latter. In particular, a PFC utilizes incident photon energy, instead of thermal energy, to produce electricity by photoelectrocatalytic degradation of the fuel. The process takes place in the presence of a semiconductor photocatalyst, which is excited by absorption of light of appropriate wavelength. In principle, oxide photocatalysts are not selective with respect to the nature of the fuel and, therefore, they are capable of degrading any organic substance in solution, including biomass-derived compounds and their derivatives, organic wastes and pollutants. Thus, PFCs may be used to convert photon energy into electricity with simultaneous mineralization of waste and/or hazardous compounds present in aqueous media. In addition, PFCs may operate at ambient conditions and they do not necessitate any sophisticated measures either for assembling or for functioning.

A simple PFC configuration [1] comprises a photoanode carrying photocatalyst, a dark cathode carrying electrocatalyst and an electrolyte. The cell is divided into two compartments separated by an ion transfer membrane. The same or different electrolytes may be introduced in the two compartments while the fuel is added only in the anode compartment [2].

As has been previously discussed [3, 4], photocatalytic oxidation of organic compounds in the presence of oxygen proceeds by utilizing not only hydroxyl radicals produced by photogenerated holes but also oxidants formed by progressive reduction of adsorbed oxygen by photogenerated electrons, such as superoxide radical $(O_2^{\bullet -})$, hydroperoxy radical

($HO_2^{\bullet}$), hydrogen peroxide (H_2O_2) and hydroxyl radical ($^{\bullet}OH$) [5–7]. Utilization of both photogenerated holes and electrons enhances the rate of oxidation of ethanol and reaction intermediates toward CO_2 but results in lower electric currents produced by the cell because less electrons are available to travel in the external circuit. This is an important issue and for this reason we have studied it in this work, seeking for ways to establish an optimal balance between the process of photodegradation-mineralization and the electric current flow. Thus the present work studies PFCs based on either pure titania photocatalyst or TiO_2 combined with metal (Pt) or metal oxide (RuO_2, NiO) co-catalysts dispersed on the semiconductor surface.

It must be underlined at this point that works of the present type [8–12] are not very frequent, even though, photocatalytic degradation by a great variety of photocatalysts are extensive and scan a range of more than 40 years. This long experience should be effectively engaged in the study of photoelectrocatalytic cells, which carry promise for future applications. Water splitting and hydrogen production can be carried out by photoelectrocatalysis and this has been repeatedly studied by many researchers [13–21]. However, the function of a PFC in the presence of a sacrificial agent, i.e. the fuel, greatly increases current and makes the process more efficient [2].

2 Experimental

2.1 Materials

Unless otherwise indicated, reagents were obtained from Aldrich and were used as received. The nanocrystalline titania employed as photocatalyst was commercial Degussa P25. Millipore water was used in all experiments. SnO_2:F transparent conductive electrodes (FTO, Resistance 8 Ω/sq) were purchased from Pilkington, USA, Carbon Cloth, 20 % wet proofing and Pt/Carbon Black electrocatalyst (30 % on Vulcan XC72) from BASF Fuel Cell, Inc., USA and Carbon Black, Vulcan XC72R, was a gift from CABOT Corporation.

2.2 Catalyst preparation and characterization

Metal-promoted photocatalysts were prepared by impregnation of TiO_2 powder with an aqueous solution of the corresponding metal precursor salt ($(NH_3)_2Pt(NO_2)_2$, $Ru(NO)(NO_3)_3$ or $(Ni(NO_3)_2{\bullet}6H_2O)$. The resulting slurry was heated slowly at 70 °C under continuous stirring, maintained at that temperature until nearly all the water evaporated, and subsequently dried at 110 °C for 24 h. Finally, ruthenium- and nickel-containing samples were calcined in air at 300 °C for 3 h to form RuO_2 and NiO crystallites, whereas the platinum-containing sample was reduced in H_2 flow (300 °C, 3 h) to obtain reduced Pt crystallites. The nominal metal loading of the catalysts was 0.5 wt% (metal basis) and was calculated on the basis of the quantities of the precursor materials. Photocatalyst powders were characterized with respect to their specific surface area (BET) employing N_2 physical adsorption (77 K). Details on the apparatus and procedures used can be found elsewhere [22].

2.3 Description of the reactor employed for photocatalytic mineralization experiments

The apparatus used for photocatalytic mineralization of ethanol has been previously described [23]. It consists of a solar light-simulating source (Osram XBO 450 W), a quartz photoreactor and a CO_2 analyzer (Binos) connected on-line at the exit of the photoreactor. In a typical experiment, a known amount of photocatalyst (80 mg) in powder form ($d < 90$ μm) is dispersed under continuous stirring in 60 ml of an aqueous solution of ethanol (10 mM). The solution temperature is adjusted at 40 °C and a flow of 20 % O_2 in He (20 cm^3 min^{-1}) is permitted through the reactor. The system is then exposed to light (at $t = 0$) and CO_2 produced by photocatalytic oxidation of ethanol is monitored continuously at the reactor effluent. The power of the incident radiation at the optical window of the reactor was measured with the use of a radiation power/energy meter (Oriel 70260) equipped with a thermopile detector probe, and was found to be 81 mW cm^{-2}.

2.4 Preparation of the anode electrode

Anode electrodes were prepared by depositing on clean FTO electrodes home-made pastes based on the powdered photocatalysts, synthesized as in Sect. 2.2. Pastes were prepared according to the recipe given in Ref. [24]. Two layers were applied giving a uniform film, which, after calcination at 550 °C, was about 8–10 μm thick [25]. The geometrical dimension of each film was $3 \times 4 = 12$ cm^2. Electric conduct was made by using an adhesive copper ribbon and a copper wire soldered on the copper ribbon.

2.5 Preparation of the cathode

Cathode electrode was made of carbon cloth with deposited Carbon Black and Pt as described in previous publications [2, 26]. An amount of 0.246 g of Carbon Black was mixed with 8 ml of distilled water by vigorous mixing in a mixer (about 2,400 rpm) until it became a viscous paste. This paste was further mixed with 0.088 ml polytetrafluoroethylene (Aldrich, Teflon 60 wt% dispersion in water) and then applied on a carbon cloth cut in the necessary dimensions. This has been achieved by first spreading the

paste with a spatula, preheating at 80 °C and finally heating in an oven at 340 °C. Subsequently, the catalytic layer was prepared as follows: 1 g of Pt/Carbon Black electrocatalyst (30 % on Vulcan XC72) was mixed with 8 g of Nafion perfluorinated resin (5 wt% solution in lower aliphatic alcohols and water, Aldrich) and 15 g of a solution made of 7.5 g H_2O and 7.5 g isopropanol. The mixture was ultrasonically homogenized and then applied on the previously prepared carbon cloth bearing carbon black. Then the electrode was heated at 80 °C for 30 min and the procedure was repeated as many times as necessary to load about 0.5 mg of Pt/cm^2. The thus prepared Pt/Carbon-Cloth (Pt/CC) electrode was ready for use. Its size was similar to the anode electrode, i.e. $3 \times 4 = 12$ cm^2.

2.6 Description of the photoelectrocatalysis reactor

We used a two-compartment reactor, which was made of Pyrex glass of cylindrical shape (55 mm internal diameter). The compartments were separated by a silica frit (ROBU, Germany, porosity SGQ 5, diameter 25 mm, thickness 2 mm). In all cases, the compartments could be tightly capped with Pyrex fittings having provisions for electrode connections and gas inlet–outlet. Each compartment could carry about 150 ml of electrolyte. The electrolyte was an aqueous solution of 0.5 M NaOH. As fuel we used 10 vol% ethanol. UVA excitation of titania was made by using Black Light fluorescent tubes, peaking around 363 nm [2]. Four tubes, each of 4 W nominal power, were placed around the anode compartment and they were covered by a cylindrical protecting-reflecting cover, having a slot that allowed the cathode compartment to be placed outside the lamp system in the dark. This reactor and excitation source configuration was very convenient for the present application, since it was not sensitive to sample direction or position in the cavity. The total radiation intensity incident on the sample was estimated to be around 3.5 mW/cm^2.

2.7 Apparatus

Electrochemical measurements were carried out with an Autolab potentiostat PGSTAT128 N. All current–voltage curves were traced at 20 mV/s. Radiation intensity was measured with a PMA 2100 Radiant Power meter (Solar Light Co), calibrated for the Near UV spectral range.

3 Results

3.1 Powdered catalysts characterization

Powdered photocatalysts, prepared as in Sect. 2.2, were characterized with respect to their BET specific surface area (SSA) and results obtained are presented in Table 1. It is observed that dispersion of metals or heat treatment at 300 °C did not practically affect SSA of the parent TiO_2 photocatalyst. It is concluded that, as far as the value of SSA is concerned, all four investigated photocatalysts were equivalent.

Table 1 Specific surface area (SSA) of powdered photocatalysts and total amount of CO_2 produced under conditions of photocatalytic oxidation of ethanol (data obtained from Fig. 2)

Photocatalyst	Pretreatment	SSA (m^2 g^{-1})	Amount of CO_2 (μmol)[a]
TiO_2 (P25)	None	41	1,268
Pt/TiO_2	Reduced with H_2 at 300 °C	37	1,270
NiO/TiO_2	Calcined in air at 300 °C	41	1,150
RuO_2/TiO_2	Calcined in air at 300 °C	40	751

[a] The stoichiometric amount expected according to reaction (1) is 1,200 μmol

3.2 Photoelectrocatalysis by employing various photocatalysts

We have studied cell operation using photoanodes made of either pure nanocrystalline titania or titania combined with a few different catalysts, namely Pt, RuO_2 and NiO. Figure 1 shows IV curves traced by using the above described cell in a two-electrode configuration (no reference electrode). As expected, based on previous results [2], the open-circuit voltage V_{oc}, i.e. the voltage at zero current,

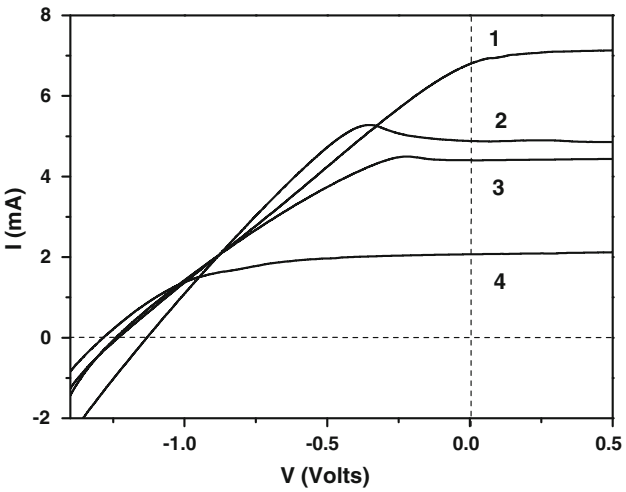

Fig. 1 IV curves for cells operating with anodes carrying various photocatalysts: *1* TiO_2, *2* Pt/TiO_2, *3* RuO_2/TiO_2, and *4* NiO/TiO_2. The electrolyte was an aerated solution of 0.5 M aqueous NaOH containing 10 %v. ethanol. The active electrode area was $3 \times 4 = 12$ cm^2. Excitation of the photocatalysts was made by UVA (Black Light) radiation

was very high, more than 1.2 V. This is one of the advantages of the PFCs running on organic fuels like ethanol and glycerol [2, 27]. V_{oc} was approximately the same for pure titania, NiO/TiO_2 and RuO_2/TiO_2 but was smaller for the Pt/TiO_2 photoanode. However, the short circuit current I_{sc}, i.e. the current at zero voltage, was the highest in the case of pure titania and substantially decreased in the presence of a co-catalyst. The lowest value of I_{sc} was observed for NiO/TiO_2. The anodic peaks appearing at −0.37 V for Pt/TiO_2 (trace *2*) and −0.26 V for RuO_2/TiO_2 (trace *3*), apparently, reveal the possibility of oxidizing Pt and Ru in these two cases. Such an anodic peak is also expected for NiO/TiO_2 but, apparently, it was very weak and thus indistinguishable.

3.3 Photoelectrocatalysis in the presence or in the absence of oxygen

The presence or the absence of oxygen in the anode compartment strongly affected the values of V_{oc} and I_{sc}. This was studied by bubbling pure oxygen or argon through the electrolyte of the anode compartment. Table 2 shows the corresponding values of the open-circuit voltage and the short-circuit current. Both V_{oc} and I_{sc} were smaller in the presence of oxygen for all the four studied cases. An obvious explanation of this behavior is that O_2 scavenges photogenerated electrons leading to the formation [7] of oxyanion radicals ($O_2^{\bullet -}$). Retaining of electrons affects both the number of available charge carriers, thus decreasing current, and the potential of the anode, making it more positive, thus decreasing V_{oc}. The results of Table 2 indicate that the cell yields more electric power in the absence of oxygen in the anode compartment.

3.4 Photocatalytic mineralization of ethanol

The photocatalytic activity of bare and metal-promoted TiO_2 catalysts for the mineralization of ethanol has been investigated in separate experiments by employing the reactor described in Sect. 2.3. The initial concentration of ethanol in the reactor was 10 mM, which was small enough to be consumed in a reasonable period of time under the present conditions. Mineralization was monitored by measuring the rate of CO_2 evolution (r_{CO_2}) at the reactor effluent as a function of irradiation time, and results obtained are summarized in Fig. 2. It is observed that, in the case of the bare TiO_2 photocatalyst, r_{CO_2} initially increases with time and then reaches a plateau of about 0.67 μmol min^{-1} (trace *a*). Evolution of CO_2 indicates that oxidation of ethanol takes place according to the following reaction:

$$C_2H_5OH + 3O_2 \rightarrow 2CO_2 + 3H_2O \quad (1)$$

Prolonged exposure to light results in an abrupt decrease of the rate of CO_2 evolution after ca 30 h, and in a practical elimination after ca 40 h of irradiation. The total amount of CO_2 produced throughout the experiment, calculated by integration of curve (*a*), was found to be 1,268 μmol (see Table 1). Considering that the initial amount of ethanol in the photoreactor was 600 μmol (60 ml, 10 mM EtOH), the stoichiometry of Eq. 1 predicts production of 1,200 μmol CO_2, which is in very good agreement with the experimental results. It may then be concluded that, under the present experimental conditions, TiO_2 is able to completely oxidize ethanol and reaction intermediates toward CO_2. When the fuel in solution was exhausted, r_{CO_2} dropped to zero (trace *a*).

Similar results were obtained over the Pt/TiO_2 photocatalyst and are shown in Fig. 2 (trace *b*). It is observed that dispersion of Pt crystallites on the semiconductor surface greatly improves photocatalytic activity for ethanol

Table 2 Values of the open-circuit voltage and the short circuit current in the presence of O_2 or Ar in the anode compartment for the four photoanodes

Photocatalyst	V_{oc} (V)		I_{sc} (mA)	
	O_2	Ar	O_2	Ar
Pure TiO_2	1.08	1.28	4.7	7.5
Pt/TiO_2	1.02	1.07	3.4	5.5
RuO_2/TiO_2	0.92	1.23	2.1	4.5
NiO/TiO_2	0.91	1.30	0.9	2.2

The active electrode area was $3 \times 4 = 12$ cm^2. Excitation of the photocatalysts was made by UVA (Black Light) radiation

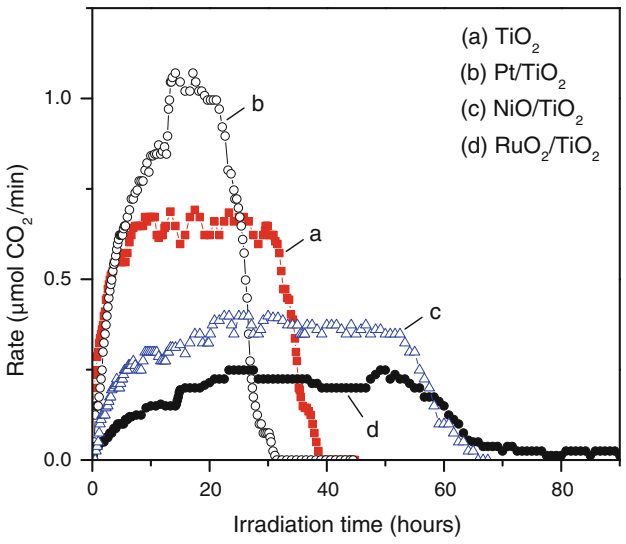

Fig. 2 Rate of CO_2 evolution as a function of irradiation time obtained over the indicated photocatalyst powders suspended in an aqueous solution of ethanol (10 mM). Excitation by simulated solar radiation

oxidation. In particular, r_{CO_2} goes through a maximum (1.06 μmol min^{-1}), which is about 60 % higher compared to that obtained for bare TiO_2. As a result, oxidation of ethanol is achieved in a much shorted period of time for the Pt-promoted photocatalyst and r_{CO_2} drops to zero after ca 30 h (Fig. 2). The opposite effect is observed when the semiconductor is loaded with nickel (trace *c*), in which case the rate maximum is substantially lower (0.40 μmol min^{-1}) and the irradiation time required for complete oxidation of ethanol is significantly larger (65 h), compared to that of bare TiO_2. Regarding the total amount of CO_2 produced over Pt/TiO_2 and NiO/TiO_2 (Table 1), it is in very good agreement with that predicted from the stoichiometry of reaction (1), indicating that both photocatalysts are able to completely oxidize ethanol and reaction intermediates into CO_2. However, this is not the case for RuO_2/TiO_2, which not only exhibits the lowest rate of CO_2 evolution (trace *d*) but is also not able to mineralize ethanol within a reasonable period of time. In particular, the total amount of CO_2 produced during 90 h under irradiation is about 60 % that expected from the stoichiometry of reaction (1) (see Table 1), indicating the inability of RuO_2/TiO_2 to efficiently catalyze the reaction.

Summarizing, the results of Fig. 2 show that Pt/TiO_2 gave the fastest fuel consumption and the highest maximum rate for ethanol oxidation. Pure titania was the next most efficient photocatalyst while Ru/TiO_2 gave the lowest reaction rates. The highest efficiency of Pt/TiO_2 was expected because of the well known ability of Pt crystallites to function as electron sink that retains electrons and impedes electron–hole recombination. It should be reminded that mineralization experiments were carried out in oxygenated solutions. Under these conditions, electrons retained by Pt can interact with O_2 to produce the highly oxidative oxyanion radical $O_2^{\bullet -}$, which adds to the oxidative power of the combined photocatalyst [3]. This function of Pt may justify the observed high mineralization rate. The consumption of the fuel (ethanol) was slower in the case of NiO/TiO_2 and even slower in the case of RuO_2/TiO_2. This is in line with previous results promoting Pt as the best Titania-loaded co-catalyst for hydrogen production under ethanol photoreforming conditions [28].

4 Discussion

It has been established since several years that combination of nanocrystalline titania with nanostructured co-catalysts dispersed on its surface results in photocatalysts with enhanced efficiency [29–33]. This may be attributed to the difference of energy levels between catalyst and co-catalyst, which induces transfer of photogenerated charge carriers from one material to the other, thus leading to efficient electron–hole separation. This is particularly true for the combination of nanocrystalline titania with noble-metal nanoparticles. Indeed, the high work function of noble metals makes them a sink that attracts and retains photogenerated electrons. However, combination with non-noble transition metals does not always make an efficient photocatalyst. There are several reasons for this diverse behavior. Metals may come in as dopants by substituting Ti lattice sites. This, however, is not easy to occur and necessitates either very high temperature treatment or sophisticated techniques of ion implantation [31, 34]. In most cases, added metals are mixed in the nanostructure and negatively affect photocatalytic performance. Thus they either create defect sites that enhance the rate of electron–hole recombination and decrease the diffusion length of the minority charge carrier [35] or they induce other unwanted effects on photocatalyst's nanostructure. A favorable case may be obtained when added metals form oxides [30, 32, 33] that are mixed with nanocrystalline titania in the nanoscale. It is then possible to transfer photogenerated holes or electrons from one photocatalyst component to the other, as already said. Still another possibility is obtained with metals like, Cr, V or Ru, which may be reduced by photogenerated electrons and thus enhance hole availability and photocatalyst oxidative power. In the present work we have made a choice of a few characteristic cases to study their influence on the function of a photoelectrocatalysis cell. According to the synthesis procedure described in Sect. 2.2, Ni and Ru are expected to come in as metal oxides, while Pt, which was reduced in a hydrogen atmosphere, was in the form of metal nanoparticles. The data of Fig. 2 show, as expected, that the presence of Pt enhanced ethanol mineralization rate. In the case of NiO/TiO_2, mineralization rate was substantially smaller than for pure titania. The failure of this oxide mixture to achieve enhanced rates may be rationalized in terms of the diagram of Fig. 3. NiO is known to be a p-type semiconductor with high-located conduction and valence band [36]. When the majority semiconductor (TiO_2) is excited, the photogenerated hole may be transferred to the higher-lying (i.e. more electronegative) valence band of NiO. However, its level is so high that it is not thermodynamically possible to activate $^{\bullet}OH$ radicals, which are considered mainly responsible for ethanol oxidation. Consequently, NiO/TiO_2 combined photocatalyst was less efficient than pure titania. Another interesting case is that of RuO_2/TiO_2. RuO_2 is considered to behave as a conductor because of its high conductivity (830 mS cm^{-1}) [39]. Its work function is also high, around 5 eV [40], comparable with that of noble metals. Thus the position of its potential in Fig. 3 is placed around +0.5 V versus NHE. RuO_2 has been studied in many works as a co-catalyst of titania for water splitting and also for oxidation of organic

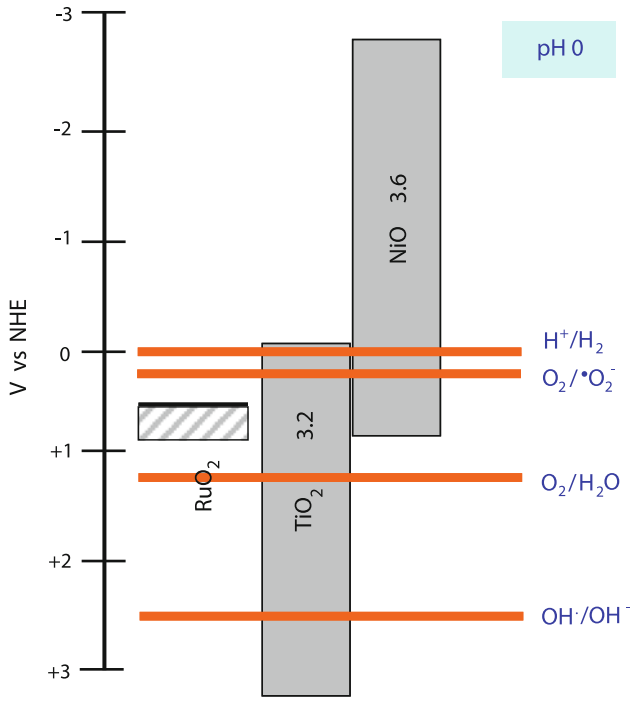

Fig. 3 Energy diagram and redox potentials for some redox couples. The values correspond to pH 0 but they may be negatively shifted by equal amounts at higher pH. Each semiconductor is presented as a parallelogram. The *upper side* corresponds to the level of the Conduction band and the *lower side* to the Valence band. The numbers in the box correspond to the band gap expressed in eV. Levels were adapted to the data found in Refs. [1, 36–38]

substances and is treated in a similar manner as noble metal co-catalysts. However, RuO_2 mainly functions as a scavenger of holes [41] while, for example, Pt acts as a scavenger of electrons. Similarly to NiO, the oxidative power of RuO_2 is not as strong as that of the valence band of pure TiO_2, as can be seen in Fig. 3, therefore, RuO_2/TiO_2 is worse photocatalyst for the mineralization of ethanol than pure titania. The above reasoning may explain the results presented in Fig. 2 and justifies the fact that Pt/TiO_2 combined photocatalyst was the best of the four choices.

The above discussion can also help to rationalise the data of Fig. 1. Pt/TiO_2 gave the smallest open-circuit voltage. This can be explained by taking into account the tendency of Pt to scavenge electrons. This means that less free electrons are found in the conduction band of titania, making it less electronegative. Hence, the drop of the (negative) voltage. The fact that voltage did not substantially change in the presence of RuO_2 and NiO is in line with the above discussed model that excited majority species (i.e. TiO_2) ejects holes and not electrons into the minority species thus preserving its electronegativity. The decrease of I_{sc}, in going from pure titania to Pt/TiO_2, is also justified by Pt electron scavenging. Thus, in the presence of Pt less electrons are available to flow through the external circuit, thereby decreasing current. We believe that the further current decrease observed in the presence of RuO_2 and NiO is simply due to the waste of energy on inefficient catalysts as far as the present system is concerned. Holes may be evacuated from excited titania in the presence of NiO or RuO_2 but they become inefficient to carry out ethanol oxidation, as already said. Therefore, they do not participate in the flow of current, which has to be done in a cyclic manner.

Another decisive factor affecting current is seen in Table 2, and is related with the presence of oxygen. Oxygen decreased both current and voltage in all studied cases. This is presumably due to the scavenging of electrons and the formation of oxyanion radicals $O_2^{\bullet -}$, as already discussed in Sect. 3.3. The presence of oxygen is necessary in order to speed up ethanol photocatalytic oxidation and mineralization. In the absence of oxygen, ethanol is going through the much slower process of photoreforming, studied by us and by others and presented in previous publications [23, 28, 42–44]. Photoreforming is usually carried out photocatalytically in a mild pH, otherwise, the aldehyde formed in an intermediate step may lead to aldol condensation [3] instead of mineralization, as already said in the Sect. 1. It is obvious that no ideal situation may be designed. Lack of oxygen or lack of an efficient mineralization photocatalyst, such as Pt/TiO_2, produces more current but creates problems. Presence of factors favoring fuel mineralization leaves less current to flow in the external circuit but assures consumption of the fuel without problems. The ideal cell may not be possible but the functional cell is.

5 Conclusions

Photoactivated fuel cells can function without any external electric bias by employing an aerated cathode. In the presence of a fuel, for example, ethanol, the open-circuit voltage can achieve very high values of 1.2 V or higher. The current depends on some crucial factors. Catalysts with low oxidative power towards the fuel, like NiO/TiO_2 and RuO_2/TiO_2, are not capable of producing high currents either. Efficient photocatalysts like Pt/TiO_2, which function by scavenging photogenerated electrons, decrease current as well. Current and voltage are always lower in the presence of oxygen, which also acts as electron scavenger but accelerates the oxidation and mineralization processes. Thus the cell should function under optimized conditions, where the oxidation–mineralization process should be favored at the partial expense of power output by the cell. In other words, the cell should function in the presence of oxygen and it is advisable to employ an efficient photocatalyst like Pt/TiO_2.

Acknowledgments This research has been co-financed by the European Union (European Social Fund—ESF) and Greek national funds through the Operational Program "Education and Lifelong Learning" of the National Strategic Reference Framework (NSRF)—Research Funding Program: Heracleitus II. Investing in knowledge society through the European Social Fund.

References

1. Lianos P (2011) J Hazard Mater 185:575
2. Antoniadou M, Lianos P (2010) Appl Catal B 99:307
3. Panagiotopoulou P, Antoniadou M, Kondarides DI, Lianos P (2010) Appl Catal B 100:124
4. Antoniadou M, Kondarides DI, Lianos P (2009) Catal Lett 129:344
5. Gerischer H, Heller A (1991) J Phys Chem 95:5261
6. Wu T, Liu G, Zhao J, Hidaka H, Serpone N (1999) J Phys Chem B 103:4862
7. Stylidi M, Kondarides DI, Verykios XE (2004) Appl Catal B 47:189
8. Kaneko M, Ueno H, Saito R, Suzuki S, Nemoto J, Fujii Y, Photchem J (2009) Photobiol A 205:168
9. Kaneko M, Suzuki S, Nemoto J, Fujii Y (2010) Electrochim Acta 55:3068
10. Seger B, Kamat PV (2009) J Phys Chem C 113:18946
11. Canterino M, Di Somma I, Marotta R, Andreozzi R, Caprio V (2009) Water Res 43:2710
12. Park H, Vecitis CD, Hoffmann MR (2009) J Phys Chem C 113:7935
13. Fujishima A, Honda K (1972) Nature 238:37–38
14. Bard AJ (1982) J Phys Chem 86:172
15. Getoff N (1990) Int J Hydrogen Energy 15:407
16. Bak T, Nowotny J, Rekas M, Sorrell CC (2002) Int J Hydrogen Energy 27:991
17. Park JH, Kim S, Bard AJ (2006) Nano Lett 6:24
18. Varghese OK (2008) C A Grimes 92:374
19. Park H, Vecitis CD, Choi W, Weres O, Hoffmann MR (2008) J Phys Chem C 112:885
20. Le Formal F, Gratzel M, Sivula K (2010) Adv Funct Mater 20:1099
21. Tode R, Ebrahimi A, Fukumoto S, Iyatani K, Takeuchi M, Matsuoka M, Lee CH, Jiang C-S, Anpo M (2010) Catal Lett 135:10
22. Panagiotopoulou P, Kondarides DI (2004) J Catal 225:327
23. Daskalaki VM, Kondarides DI (2009) Catal Today 144:75
24. Ito S, Chen P, Comte P, Nazeeruddin MK, Liska P, Pechy P, Gratzel M (2007) Prog Photovolt Res Appl 15:603
25. Antoniadou M, Stathatos E, Boukos N, Stefopoulos A, Kallitsis J, Krebs FC, Lianos P (2009) Nanotechnology 20:495201
26. Antoniadou M, Kondarides DI, Labou D, Neophytides S, Lianos P (2010) Sol Energy Mater Sol Cells 94:592
27. Antoniadou M, Lianos P (2011) Photochem Photobiol Sci 10:431
28. Strataki N, Bekiari V, Kondarides DI, Lianos P (2007) Appl Catal B 77:184
29. Sakata T, Kawai T (1981) Chem Phys Lett 80:341
30. Vinodgopal K, Bedja I, Kamat PV (1996) Chem Mater 8:2180
31. Ohno T, Tanigawa F, Fujihara K, Izumi S, Matsumura M (1999) J Photochem Photobiol A Chem 127:107
32. Gao Y-L, Chen Q-Y, Tong H-X, Hu H-P, Qian D, Yang Y-H, Zhou J-L (2009) J Cent South Univ Technol 16:919
33. Nakhate GG, Nikam VS, Kanade KG, Arduj S, Kale BB, Baeg JO (2010) Mater Chem Phys 124:976
34. Kitano M, Matsuoka M, Ueshima M, Anpo M (2007) Appl Catal A General 325:1
35. Di Paola A, Marci G, Palmisano L, Schiavello M, Uosaki K, Ikeda S, Ohtani B (2002) J Phys Chem B 106:637
36. He J, Lindstrom H, Hagfeldt A, Lindquist S-E (1999) J Phys Chem B 103:8940
37. Fujishima A, Zhang X, Tryk DA (2007) Int J Hydrogen Energy 32:2664
38. Nozik AJ (1978) Ann Rev Phys Chem 29:189
39. Chervin CN, Lubers AM, Long JW, Rolison DR (2010) J Electroanal Chem 644:155
40. Park CS, Bersuker G, Hung PY, Kirsch PD, Jammy R (2010) Electrochem Solid-State Lett 13:H105
41. Kalyanasundaram K, Gratzel M, Pelizzetti E (1986) Coordin. Chem Rev 69:57
42. Patsoura A, Kondarides DI, Verykios XE (2007) Catal Today 124:94
43. Kondarides DI, Daskalaki VM, Patsoura A, Verykios XE (2008) Catal Lett 122:26
44. Kondarides DI, Patsoura A, Verykios XE (2010) J Adv Oxid Technol 13:116